2022-10-01

Punching Shear Capacity of Recycled Aggregate Concrete Slabs

Leelatanon, S

10.3390/buildings12101584
Buildings
MDPI AG

buildings

MDPI

Article

Punching Shear Capacity of Recycled Aggregate Concrete Slabs

Satjapan Leelatanon [1], Thanongsak Imjai [1], Monthian Setkit [1,*], Reyes Garcia [2] and Boksun Kim [3]

Accepted on Sep. 21, 2022.

Published on Oct. 1, 2022.

Buildings **2022**, *12*, 1584. https://doi.org/10.3390/buildings12101584

[1] Center of Excellence in Sustainable Disaster Management, School of Engineering and Technology, Walailak University, Nakhon Si Thammarat 80160, Thailand; lsatjapa@wu.ac.th (S.L.); thanongsak.im@wu.ac.th (T.I.)

[2] Civil Engineering Stream, School of Engineering, The University of Warwick, Coventry CV4 7AL, UK; reyes.garcia@warwick.ac.uk

[3] School of Engineering, Computing and Mathematics, University of Plymouth, Plymouth PL4 8AA, UK; boksun.kim@plymouth.ac.uk

* Correspondence: smonthia@wu.ac.th; Tel.: +66-(0)-7567-2385

Abstract: This article investigates the punching shear behavior of recycled aggregate concrete (RAC) two-way slabs. Ten 1500 mm × 1500 mm × 100 mm slabs were tested monotonically. Eight slabs were cast with RAC, whereas two control slabs were cast with natural aggregate concrete (NAC). The RAC incorporated coarse recycled concrete aggregate (RCA) at replacement levels of 25%, 50%, 75% and 100%. Two flexural reinforcement ratios (0.8% and 1.5%) were examined. The results show that the normalized punching shear strength of 100% RAC slabs decreased by 6.5% and 9% compared to NAC slabs for $\rho = 1.5\%$ and $\rho = 0.8\%$, respectively. Doubling the amount of flexural reinforcement can increase the punching shear capacity of 100% RAC slabs by up to 45%. A punching shear database of 44 RAC slabs from literature and the 8 RAC slabs presented in this study revealed that the punching shear strength of RAC slabs predicted by ACI 318 was conservative, except for slabs with low reinforcement ratios (<0.6%). The punching shear strength predicted by Eurocode 2 gave more conservative results for all levels of RCA replacement and all flexural reinforcement ratios. A yield-line analysis also showed that the failure mode of the RAC slabs was controlled by punching shear.

Keywords: recycled aggregate concrete; punching shear; two-way slabs; slab–column connection; flexural reinforcement ratios; yield-line analysis

Citation: Leelatanon, S.; Imjai, T.; Setkit, M.; Garcia, R.; Kim, B. Punching Shear Capacity of Recycled Aggregate Concrete Slabs. *Buildings* **2022**, *12*, x. https://doi.org/10.3390/xxxxx

Academic Editor(s): Pavel Reiterman

Received: 1 September 2022
Accepted: 21 September 2022
Published: date

1. Introduction

Concrete is a primary construction material widely used in construction around the world. Demand for concrete keeps growing each year to meet the rapid economic and population growth, leading to increasing demands in natural aggregate production. The consumption of natural aggregate worldwide was approximately 48.3 billion tonnes in 2015, and the demand is expected to double in the next two or three decades [1]. The extraction of aggregates from quarries and riverbeds poses several environmental issues, such as air and water pollution, destruction of natural habitats, as well as natural resource depletion. For these reasons, the construction industry is pushing towards more sustainable construction to minimize these environmental problems [2].

Numerous studies have focused on finding more sustainable and efficient use of materials in concrete, particularly on using alternative materials (such as waste glass and waste plastics) to substitute fine and coarse aggregates. For instance, plastic waste caps as coarse aggregates [3] or PET waste particles as sand replacement [4] have been used in reinforced concrete beams. However, the sustainability of the plastic industry itself is under heavy scrutiny, and thus this industry is unlikely to meet the demand for aggregates.

Besides the issue of natural resource depletion, another issue in the construction industry is construction and demolition waste (CDW). In the past, CDW has been primarily downgraded, or even dumped in open landfills. However, since the largest constituent of

concrete is coarse aggregate (which counts for approximately 60% of the concrete volume), efforts on reusing recycled aggregate concrete (RAC) have increased worldwide, especially in developed countries such as the USA, Europe, Japan, as well as China, where environmental concerns in construction are at the top of their agendas [5–7].

To date, most of the actual applications of RAC are limited to non-structural purposes (such as backfills and road sub-bases) due to skepticism and lack of suitable design guidelines for structural members. Although several research works have studied the structural behavior of RAC beams under flexure [8–15] and shear [16–39], some results are still contradictory. This is especially true regarding the shear strength of members, where the physical variations of coarse recycled concrete aggregate (RCA) influence the response, and this has led to skepticism towards the real structural applications of RAC.

The shear behavior of reinforced concrete members is complex. Shear predictions of such members are generally based on empirical formulae derived from a large test data set. Whilst research on shear of RAC beams exists, studies on the punching shear of RAC slabs are limited. Presenting the first report on punching shear capacity, Rao et al. [40] tested 15 RAC and 3 NAC slabs by varying the replacement levels of RCA from 0%, 20%, 40%, 60%, 80%, and 100%. All slabs had dimensions of 1100 × 1100 × 50 mm and a constant 0.63% flexural reinforcement. Their findings indicate that the punching shear capacity of 100% RCA decreased by 14.1% compared to that of an equivalent NAC slab.

RAC slab tests were also conducted by Reis et al. [41] on eight specimens with 0%, 20%, 50%, and 100% RCA and 0.93% of the flexural reinforcement ratio. They found that RCA did not affect the punching shear capacity of the tested slabs, but instead it decreased the initial stiffness and cracking load. Francesconi et al. [42] conducted the experimental investigation of 12 slabs with RCA with replacement levels ranging from 30%, 50%, 80%, and 100%, and a flexural reinforcement ratio of 0.56%. Their results indicate that punching shear strengths of all RAC slabs were similar to those of NAC slabs.

Mahmoud et al. [43] investigated the punching shear behavior of RAC slabs with 0%, 30%, 60%, and 100% and two sizes (12.5 and 25 mm) of RCA. The authors reported that punching shear decreased as the replacement of NCA with RCA increased. Xiao et al. [44] also tested RAC slabs with and without steel fibers. Their findings indicated that the punching shear capacity of RAC slabs without fibers, ductility, and energy dissipation decreased with increasing levels of RCA replacement.

Sahoo et al. [45] performed 18 punching shear tests of RAC slab–column connections with 0%, 50%, and 100% RCA. The authors concluded that punching shear capacities were practically independent of RCA replacement levels. They also proposed a simple strut-and-tie model to predict the punching shear strength of RAC slabs.

In most previous studies, the RCA replacement levels were the main variable, with much focus on medium- and high-strength concrete. To date, the effect of varying the amount of flexural reinforcement to increase the punching shear of RAC slabs has not been studied. Therefore, the present study focuses on examining normal concrete strength (20–30 MPa) as well as the effect of doubling the flexural reinforcement ratios (from 0.8% to 1.5%).

To achieve this, ten slabs were tested monotonically. Eight of such slabs were cast with RAC, whereas two control slabs were cast with NAC. The RAC incorporates coarse RCA at replacement levels of 25%, 50%, 75% and 100%. These parameters were then examined using a punching shear database from RAC slabs available in the literature, and subsequently compared against the punching shear equations included in ACI 318 [46] and Eurocode 2 [47].

ACI 318 and Eurocode 2 were selected in this study since these are internationally recognized codes widely used in design practice. This study contributes towards developing more accurate design guidelines for RAC slabs, which in turn is expected to promote a more efficient use of recycled materials in construction.

2. Experimental Investigation

2.1. Material Properties

The concrete mixtures were designed to have a target 28-day compressive strength of 28 MPa. The mixtures included Type 1 Ordinary Portland Cement (OPC), natural coarse aggregate (NCA), recycled concrete aggregate (RCA), fine aggregate, water, and superplasticizer. The RCA was sourced from waste concrete cylinders with a compressive strength of approximately 30 MPa (see Figure 1a). The concrete waste was less than one year old and was from a nearby construction. All concrete cylinders were crushed by a custom-made crushing machine, as shown in Figure 1b.

(**a**) (**b**) (**c**)

Figure 1. (**a**) Concrete waste cylinders, (**b**) crushing machine, and (**c**) RCA obtained from concrete waste cylinders.

The NCA and RCA used in this study had a maximum size of approximately 19 mm, which is the typical maximum size used in concrete for structural elements in Thailand. Figure 1c shows the RCA used in this study. The specific gravity and water absorption of the RCA were 2.43 and 4.59%, respectively, while the corresponding values of NCA were 2.7 and 0.28%. Sieve analysis of coarse and fine aggregates was conducted in accordance with ASTM C136 [48], and the corresponding results are shown in Figure 2. The properties of coarse and fine aggregates are summarized in Table 1.

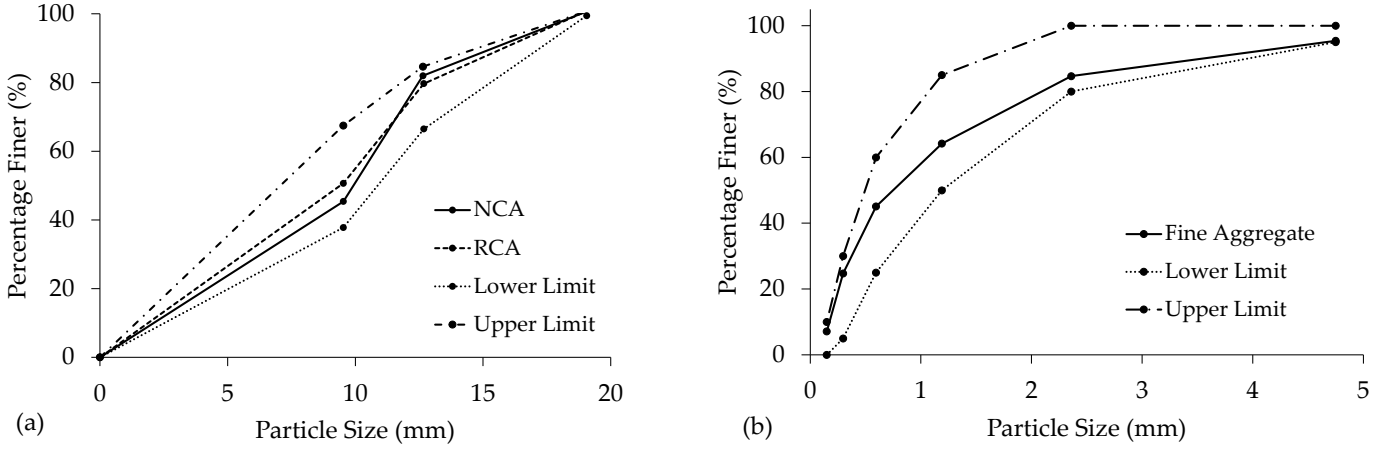

Figure 2. Gradation curves for (**a**) coarse aggregates and (**b**) fine aggregates.

Table 1. Properties of fine aggregate (FA), natural coarse aggregate (NCA), and coarse recycled concrete aggregate (RCA).

Properties	FA	NCA	RCA
Bulk Specific Gravity (SSD)	2.6	2.7	2.43
Unit Weight (kg/m^3)	-	1730	1397
Water Absorption (%)	1.05	0.28	4.59
Moisture (%)	1.35	0.61	2.24
Fineness Modulus	2.7	-	-
Max. size (mm)	4.76	19.1	18.6
Impact value (%)	-	10.15	13.4
Crushing value (%)	-	21.77	23.12

The steel reinforcement used in all specimens consisted of deformed rebars with a 12 mm diameter. Five coupons were randomly selected for tensile tests to determine the average yield and ultimate strength of the reinforcing bars. The yield and ultimate strengths of the rebars were 568 and 660 MPa, respectively. All the steel reinforcement came from a single batch.

2.2. Concrete Mix Proportions

The concrete mix proportions were calculated according to ACI 211.1 [49] adopting a water–cement ratio of 0.5. In all mixes, the NCAs were substituted by RCA at volumetric substitution levels of 25%, 50%, 75% and 100%. Table 2 shows the five concrete mix proportions used in this study. Superplasticizer (SP) was added to improve workability in both NCA and RCA mixes.

Table 2. Concrete mix proportions (in kg/m^3).

Mix Type	Cement	FA	NCA	RCA	Water	SP
NCA	357	719	1069	-	190	1.07
25% RCA	357	750	802	216	190	1.07
50% RCA	357	780	535	432	190	1.07
75% RCA	357	810	267	648	190	1.07
100% RCA	357	840	-	864	190	1.07

Note: FA = fine aggregate, NCA = natural coarse aggregate, RCA = coarse recycled concrete aggregate, and SP = superplasticizer.

2.3. Details of Slab Specimens

Figure 3a shows the geometry in plan of the tested slabs. All slabs had dimensions of 1500 × 1500 × 100 mm. A 200 × 200 mm column stub was placed at the center of each slab for load application. The slabs were supported by beams along their perimeter to simulate a simply supported condition. This led to a clear span of 1300 mm. The slabs were tested in an upside-down configuration. The vertical actuator fixed to the steel frame was used to apply load on the column stubs, as shown in Figure 3b. The slab dimension (i.e., 1500 mm) was chosen to fit the testing frame, whose clear space was 1800 mm only.

The slabs were designed to ensure that a punching shear failure occurred before a flexural failure. Accordingly, a yield-line analysis (as explained in Appendix A) was performed to predict the flexural failure load. The punching shear load was then calculated using ACI 318-19 to ensure that such shear load was lower than the yield-line load.

The slabs were categorized into two groups based on the flexural reinforcement ratios. A slab thickness of 100 mm was selected so as to obtain two flexural reinforcement ratios of 0.8% and 1.5%. Such ratios ensured a punching shear failure before a flexural failure and allowed us to experimentally investigate their impacts on the punching shear capacities of the RAC slabs. The flexural reinforcement ratio of eight 12 mm rebars with 200 mm spacing was installed in the first group of slabs (see Figure 4a), resulting in the flexural reinforcement ratio of 0.8%. This flexural reinforcement ratio is within typical values in the column strips of the flat plate in the light-load buildings [50].

In the second group of slabs, fifteen 12 mm steel bars were spaced at 100 mm to form the reinforcement ratio of 1.5% (Figure 4b), which is the maximum amount of reinforcement permitted by ACI 318 for flexural resistance. The average effective depth for all slab specimens was 73 mm. Details of the reinforcement layout are depicted in Figure 4a,b. All slabs were cast in steel formworks and tested after 28 days of casting. Likewise, six 150 × 300 mm (diameter × height) cylinders from each batch were cast and tested to obtain the concrete compressive strength on the same day the punching shear tests were carried out.

The nomenclature of the RAC slabs started with 'RCA' followed by their RCA percentages. The spacing of flexural reinforcement was at the end of the nomenclature. For instance, RCA-0-10 was a slab without RCA and with a reinforcement ratio of ρ = 1.5%. Conversely, nomenclature RCA-50-20 indicated that the slab incorporated 50% RCA and that the flexural reinforcement was ρ = 0.8%.

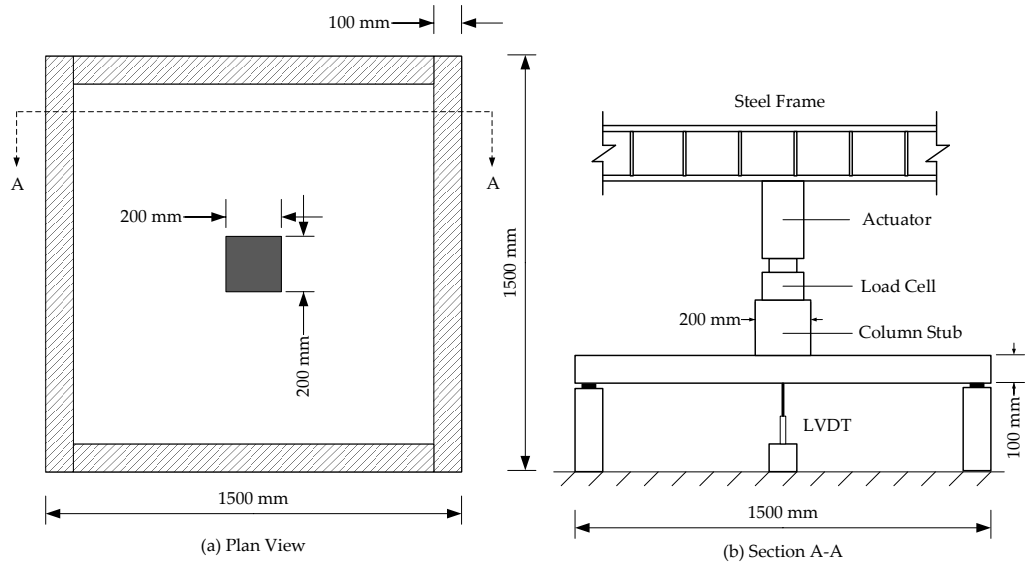

Figure 3. Dimensions of slabs: (**a**) plan view; (**b**) test setup.

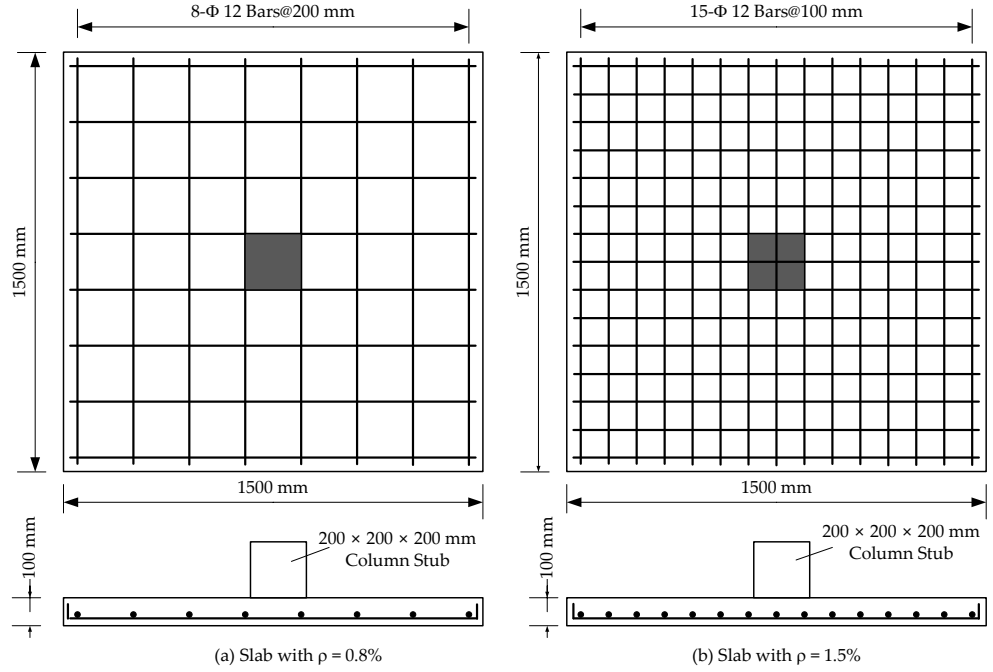

Figure 4. Details of reinforcement layout: (**a**) slabs with ρ = 0.8%; (**b**) slabs with ρ = 1.5%.

2.4. Test Setup and Testing Procedure

The load was applied by a hydraulic actuator attached to a load cell of 1000 kN. The slabs were supported on beams along the perimeter to simulate a simply supported condition. Two linear variable differential transformers (LVDTs) of 50 mm were installed under the slabs at the center of the column stub to monitor the deflections of the slabs. A data acquisition system (KYOWA EDX-10 Series) monitored and recorded the applied load and slab deflections throughout the tests. The load was applied continuously until the slabs failed. On the testing day, six concrete cylinders were also tested to determine the average compressive strength of the concrete.

3. Results and Discussion

3.1. Observed Damage

As expected, the slabs failed in brittle modes caused by punching shear. At the top of the slabs, the column stubs were punched through the slabs, as shown in Figure 5. After the tests, the slab specimens were flipped over, and crack patterns were marked. Punching shear cracking was clearly observed at the bottom of slabs. It is evident that the slabs with a reinforcement ratio of 0.8% showed more severe cracked areas at the bottom than those with a 1.5% reinforcement ratio, as illustrated in Figures 6 and 7.

Figure 5. Penetration of column at the top surface of slabs.

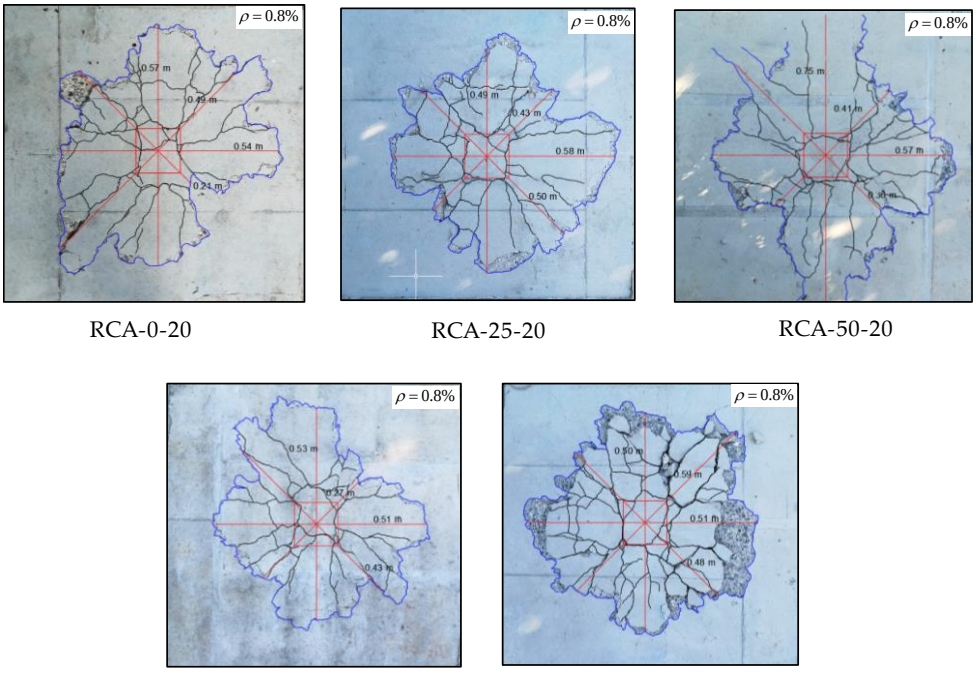

RCA-0-20 RCA-25-20 RCA-50-20

RCA-75-20 RCA-100-20

Figure 6. Punching shear failure patterns at the bottom of slabs with ρ = 0.8%.

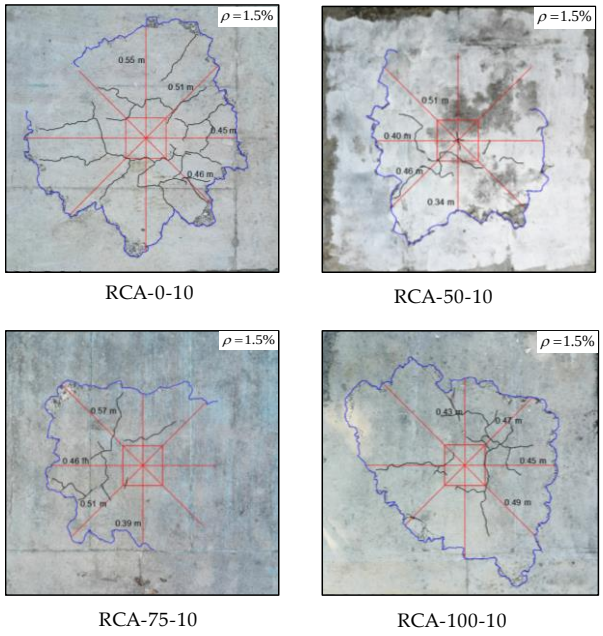

Figure 7. Punching shear failure patterns at the bottom of slabs with ρ = 1.5%.

For the slab series with a 0.8% reinforcement ratio (Figure 6), the large crack area had an average radius of approximately 500 mm from the center of the column stub. Cracks propagated from the center under the columns through the edges of slabs. The largest crack widths (that measure more than 1 mm) were observed in these slabs. The punching shear failure patterns for RAC slabs were similar to those of NAC slabs.

For slabs in the series of a 1.5% reinforcement ratio (Figure 7), the crack propagation was less severe because more flexural reinforcement helped increase the shear capacity of the slabs and hence this restrained crack development. The measured crack widths in these slabs were less than 0.5 mm. Unlike damage patterns of slabs in the first series, only a few cracks were observed before punching shear failure occurred.

3.2. Load-Deflection Response

Figure 8a,b show the load–deflection response of the slabs. All slabs had an initial linear stiffness until the first cracking occurred under the column, thus leading to stiffness degradation. With increasing load after first cracking, nonlinear load–deflection responses followed due to more cracks forming at the slabs' bottom, which also propagated towards the edges. Punching shear failure suddenly occurred when the peak load was reached. Table 3 summarizes the experimental results of the tested slabs.

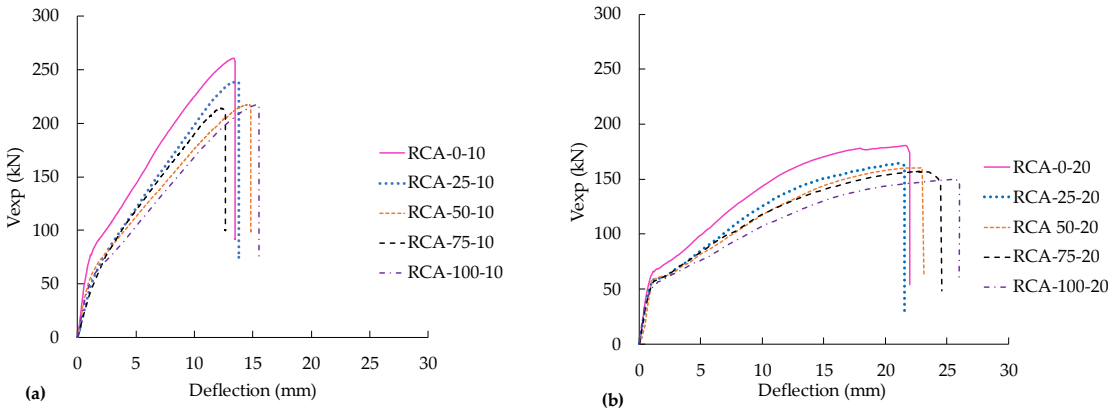

Figure 8. Load–deflection curves: (**a**) slabs with ρ = 1.5%; (**b**) slabs with ρ = 0.8%.

Table 3. Summary of experimental results of tested slabs.

Specimen	RCA Replacement (%)	ρ (%)	f'_c (MPa)	V_{cr} (kN)	V_{exp} (kN)	Δ_u (mm)	$\frac{V_{exp}}{\sqrt{fc'}b_0d}$ (MPa)	Energy Absorption (kN-mm)
RCA-0-10	0	1.5	28.1	76.8	260.9	13.5	0.62	2266
RCA-25-10	25	1.5	27.2	70.0	245.3	13.8	0.59	2014
RCA-50-10	50	1.5	24.3	62.0	217.8	14.8	0.55	2060
RCA-75-10	75	1.5	23.1	61.0	214.8	12.7	0.56	1715
RCA-100-10	100	1.5	22.2	59.0	217.5	15.5	0.58	2113
RCA-0-20	0	0.8	26.5	65.1	180.0	22.0	0.44	2999
RCA-25-20	25	0.8	24.5	58.5	164.0	21.6	0.42	2565
RCA-50-20	50	0.8	23.5	57.6	159.8	23.1	0.41	2674
RCA-75-20	75	0.8	24.1	58.1	156.9	24.5	0.40	2868
RCA-100-20	100	0.8	22.3	54.2	150.4	26.0	0.40	2915

Note: ρ = longitudinal reinforcement ratio, f'_c = cylinder concrete compressive strength on day of punching shear test, V_{cr} = first cracking load, V_{exp} = ultimate punching shear load, Δ_u = deflection at failure.

The cracking loads were approximately 29% and 36% of the peak loads for slabs with ρ = 1.5% and 0.8%, respectively. Figure 8 shows that the cracking loads and punching shear capacity decreased with increasing levels of RCA replacement. In general, the stiffness after first cracking followed the same trend, where the stiffness decreased with increasing levels of RCA replacement. This can be attributed to the lower modulus of elasticity of RAC. The overall stiffness after the first cracks of the slabs with ρ = 1.5% was obviously higher than that of slabs with ρ = 0.8%, as shown in Figure 8, which in turn confirmed the contribution of flexural reinforcement to the stiffness of the slabs.

The maximum deflections (Δ_u) measured under the column are shown in Table 3. Generally, the ultimate deflections increased with increasing levels of RCA. The deflections of 100% RCA slabs were 15% and 18% higher than those of the control NCA slabs for ρ = 1.5% and 0.8%, respectively. It can be observed that doubling flexural reinforcement can decrease the deflection of 100% RCA slabs by 68%.

Table 3 also presents the energy absorption, which is calculated here as the area under load–deflection curves shown in Figure 8a,b. The relationship between RCA contents and the energy absorption of slabs with ρ = 1.5% was unclear. For slabs with ρ = 0.8%, the energy absorption increased when NCA was substituted by 25%, 50%, 75%, and 100% RCA. Most of the energy absorption in this study was in the range of 2000–3000 kN-mm, which is similar to the RAC slabs with normal compressive strength tested by Sahoo and Singh [45].

Figure 9 shows the relationship between the punching shear stresses (V_{exp}/b_od) normalized by the square root of the concrete compressive strength, and the vertical deflection at the middle of the slabs. The perimeter b_o was determined based on the recommendation of ACI 318 [46], located at d/2 from the faces of the column. The term d was the average effective depth of flexural reinforcement, which was 73 mm in this study. These graphs allow for the comparison of punching shear capacity with different concrete compressive strengths.

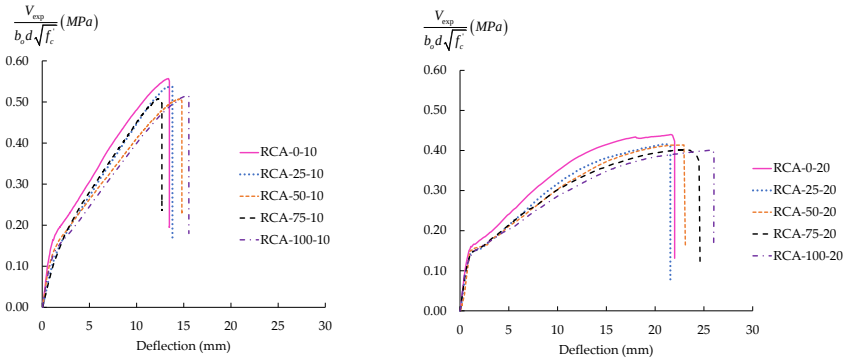

Figure 9. Normalized shear stresses vs. deflection curves: (**a**) slabs with ρ = 1.5%; (**b**) slabs with ρ = 0.8%.

It was found that the differences of normalized punching shear capacity between the controlled slabs and 100% RCA slabs were 6.5% and 9% for slabs with ρ = 1.5% and ρ = 0.8%, respectively. These plots show that the normalized punching shear strengths were higher than 0.33 (the shear strength factor in the ACI 318 provision), thus indicating that the punching shear capacities of the RAC slabs were conservative. The normalized shear strengths range from 0.58 to 0.62 and 0.40 to 0.44 for slabs with ρ = 1.5% and 0.8%, respectively. From the tested results of the 100% RCA slabs, the punching shear strength of the slabs with ρ = 1.5% increased by 45% compared to the slabs with ρ of 0.8%. This increased normalized punching shear strength indicates that the flexural reinforcement plays a vital role in the punching shear strength of the slab–column connections.

3.3. Punching Shear Failure Loads and Comparison with ACI 318-19 and Eurocode 2

To evaluate the accuracy of international design codes at predicting the punching shear strength of slab–column connections, the experimental punching shear is divided by the shear predictions by ACI 318 and Eurocode 2 to give the punching shear strength ratios, as summarized in Table 4. A summary of the punching shear strengths by ACI 318-19 [46] and Eurocode 2 [47] provisions are provided in Appendix A. The calculations of the punching shear strengths in Table 4 are carried out without material safety factors.

Table 4. Comparison of the test results with ACI 318-19 and Eurocode 2 predictions.

Specimen	V_{exp} (kN)	V_{ACI} (kN)	V_{exp}/V_{ACI}	V_{EC2} (kN)	V_{exp}/V_{EC2}
RCA-0-10	260.9	139.45	1.87	199.9	1.30
RCA-25-10	245.3	137.20	1.79	197.8	1.24
RCA-50-10	217.8	129.68	1.68	190.5	1.14
RCA-75-10	214.8	126.43	1.70	187.3	1.15
RCA-100-10	217.5	123.95	1.76	188.4	1.16
RCA-0-20	180.0	135.42	1.33	159.0	1.13
RCA-25-20	164.0	130.21	1.26	154.9	1.06
RCA-50-20	159.8	127.52	1.25	152.8	1.05
RCA-75-20	156.9	129.14	1.22	154.9	1.02
RCA-100-20	150.4	124.23	1.21	149.5	1.01

From the results in Table 4, it is evident that both provisions give the conservative shear strength ratios regardless of the RCA contents. However, comparing slabs with 100% RCA and the control ones (NAC slabs), the punching shear strength ratios predicted by ACI 318-19 decreased by 5.88% (from 1.87 to 1.76) and 9% (from 1.33 to 1.21) for slabs with ρ = 1.5% and 0.8%, respectively. Conversely, the punching shear strength ratios calculated by Eurocode 2 (EC2) for slabs 100% RCA and 0% RCA yield similar trends, where slabs with 100% RCA have the lowest punching shear strength ratios by 10.8% (from 1.30 to 1.16) and 10.6% (from 1.13 to 1.01) for ρ = 1.5% and 0.8%, respectively.

The punching shear strength ratios by Eurocode 2 for all slabs are higher than 1, thus indicating the conservativeness of the predictions. Comparing the shear strength ratios to those of ACI 318-19, Eurocode 2 gives more accurate results with ratios between 1.01 and 1.30 against 1.21 and 1.87 from ACI 318-19. The better accuracy of Eurocode 2 is partly attributed to the inclusion of the flexural reinforcement ratio in the shear equation.

3.4. Prediction of Shear Strength Ratios using Extended Dataset

Based on extensive research on the mechanical properties of RAC, it can be concluded that its inferior properties reduced the strength and performance of structural members made using recycled aggregates. In the case of punching shear, the applicability of two recognized international design codes is evaluated by test data available in the existing

literature. Forty-four slab tests published in past studies and the eight slab specimens presented in this study were investigated. All slabs were cast with RCA obtained from old concrete. The test results are summarized in Table 5.

Table 5. Comparison of punching shear capacities vs. ACI 318-19 and Eurocode 2.

Authors	Specimen	RCA (%)	ρ (%)	d (mm)	f_c' (MPa)	V_{exp} (kN)	$V_{exp}/V_{ACI\ 318}$	V_{exp}/V_{EC2}
This study	RCA-25-100	25	0.8	73	27.2	245.3	1.79	1.24
	RCA-50-100	50	0.8	73	24.3	217.8	1.68	1.14
	RCA-75-100	75	0.8	73	23.1	214.8	1.70	1.15
	RCA-100-100	100	0.8	73	22.2	217.5	1.76	1.16
	RCA-25-200	25	1.5	73	24.5	164.0	1.26	1.06
	RCA-50-200	50	1.5	73	23.5	159.8	1.25	1.05
	RCA-75-200	75	1.5	73	24.1	156.9	1.22	1.02
	RCA-100-200	100	1.5	73	22.3	150.4	1.21	1.01
Sahoo at al. [45]	N50-1	50	1.16	75	28.4	211.5	1.76	1.58
	N50-2	50	1.16	75	28.4	217.0	1.81	1.63
	N100-1	100	1.16	75	29.4	218.9	1.80	1.62
	N100-2	100	1.16	75	29.4	230.0	1.89	1.70
	M50-1	50	1.16	75	43.5	252.6	1.70	1.64
	M50-2	50	1.16	75	43.5	255.8	1.72	1.66
	M100-1	100	1.16	75	43	257.1	1.74	1.68
	M100-2	100	1.16	75	43	260.1	1.76	1.70
	H50-1	50	1.16	75	56.8	252.4	1.49	1.50
	H50-2	50	1.16	75	56.8	267.5	1.57	1.59
	H100-1	100	1.16	75	58.0	263.4	1.53	1.55
	H100-2	100	1.16	75	58.0	270.4	1.57	1.59
Xiao et al. [44]	RAC30-0%	30	1.14	99	36.34	313.4	1.33	1.23
	RAC50-0%	50	1.14	99	31.16	307.1	1.41	1.27
	RAC100-0%	100	1.14	99	29.64	303.4	1.43	1.28
Mahmoud et al. [43]	RCA-30%-12.5	30	1.12	70	34.5	153.0	1.66	1.22
	RCA-60%-12.5	60	1.12	70	32.5	137.5	1.53	1.11
	RCA-100%-12.5	100	1.12	70	31.6	122.0	1.38	1.00
	RCA-30%-25	30	1.12	70	36.4	157.0	1.66	1.23
	RCA-60%-25	60	1.12	70	34.1	140.5	1.53	1.12
	RCA-100%-25	100	1.12	70	33.6	131.0	1.44	1.05
Francesconi et al. [42]	RC1-1	30	0.56	35	63.6	64.9	0.87	1.27
	RC1-2	30	0.56	35	63.6	72.5	0.97	1.42
	RC1-3	30	0.56	35	63.6	72.5	0.97	1.42
	RC2-1	50	0.56	35	62.0	64.9	0.88	1.28
	RC2-2	50	0.56	35	62.0	68.7	0.93	1.36
	RC2-3	50	0.56	35	62.0	64.9	0.88	1.28
	RC3-1	80	0.56	35	56.3	68.7	0.98	1.40
	RC3-2	80	0.56	35	56.3	64.9	0.92	1.33
	RC3-3	80	0.56	35	56.3	72.5	1.03	1.48
	RC4-1	100	0.56	35	50.8	68.7	1.03	1.45
	RC4-2	100	0.56	35	50.8	68.7	1.03	1.45
	RC4-3	100	0.56	35	50.8	72.5	1.09	1.53
Reis et al. [41]	C20-1	20	0.93	72	35.1	158.6	1.35	1.27
	C20-2	20	0.93	72	35.1	152.2	1.30	1.22
	C50-1	50	0.93	72	36.9	163.6	1.36	1.29
	C50-2	50	0.93	72	36.9	174.8	1.45	1.38
	C100-1	100	0.93	72	36.2	161.8	1.36	1.28
	C100-2	100	0.93	72	36.2	158.3	1.33	1.26
Rao et al. [40]	RCAC-20-S	20	0.63	34	33.5	47.2	1.36	1.34
	RCAC-40-S	40	0.63	34	32.4	45.8	1.34	1.31
	RCAC-60-S	60	0.63	34	30.9	44.6	1.33	1.30
	RCAC-80-S	80	0.63	34	28.4	42.8	1.34	1.28
	RCAC-100-S	100	0.63	34	26.4	41.4	1.34	1.27
Mean							1.39	1.34
Standard Deviation							0.29	0.20

The first parameter that could have affected punching shear capacity is the content of RCA. Based on test results from Rao et al. [40], Mahmoud et al. [43], Xiao et al. [44], and this study, it was found that the ultimate punching shear capacity reduced with increasing replacement levels of RCA. These results contradict the findings by Reis et al. [41], Francesconi et al. [42], and Sahoo and Singh [45], where the punching shear strength was insensitive to RCA replacement levels.

Despite this inconsistency, the punching shear strength ratios between experimental work and predictions by ACI 318-19 and Eurocode 2 are still higher than 1 in most tests, as confirmed in Figures 10a and 11a. Even at a 100% RCA replacement level, slabs can resist punching load more than what both codes predict. However, ACI 318 gives a lower prediction of punching shear in six of the tested slabs, as shown in Figure 10a. These unconservative results come from slabs tested by Francesconi et al. [42], where the flexural reinforcement ratio is 0.56%, as depicted in Figure 10b. Since ACI 318-19 does not include the effect of flexural reinforcement in the equations, the punching shear strength of slabs with a low flexural reinforcement ratio below 0.7% could be unsafe [50]. On the other hand, the predictions by Eurocode 2 (which includes flexural reinforcement ratio in the expression) give more conservative results, as depicted in Figure 11b.

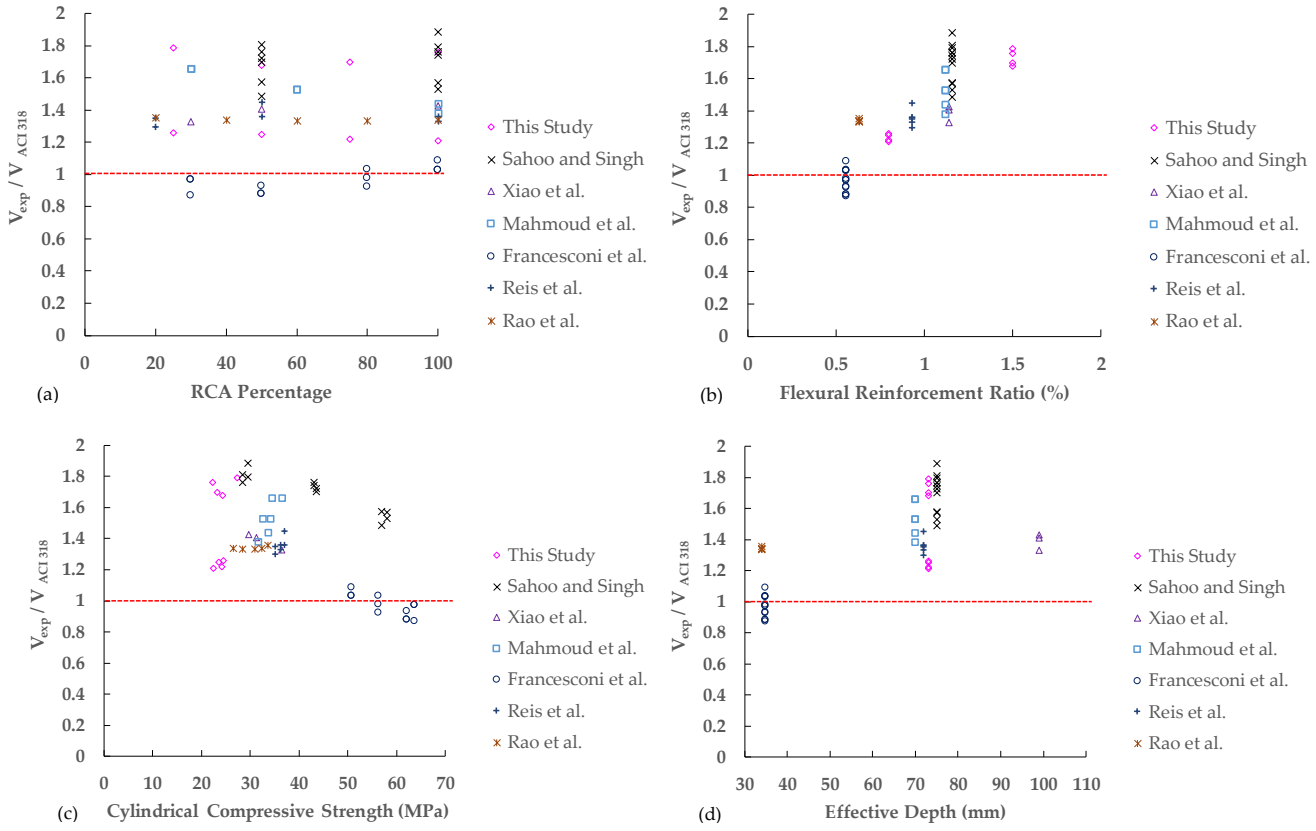

Figure 10. ACI 318 punching shear strength ratios versus (**a**) RCA percentage, (**b**) flexural reinforcement ratio, (**c**) cylindrical compressive strength, and (**d**) effective depth.

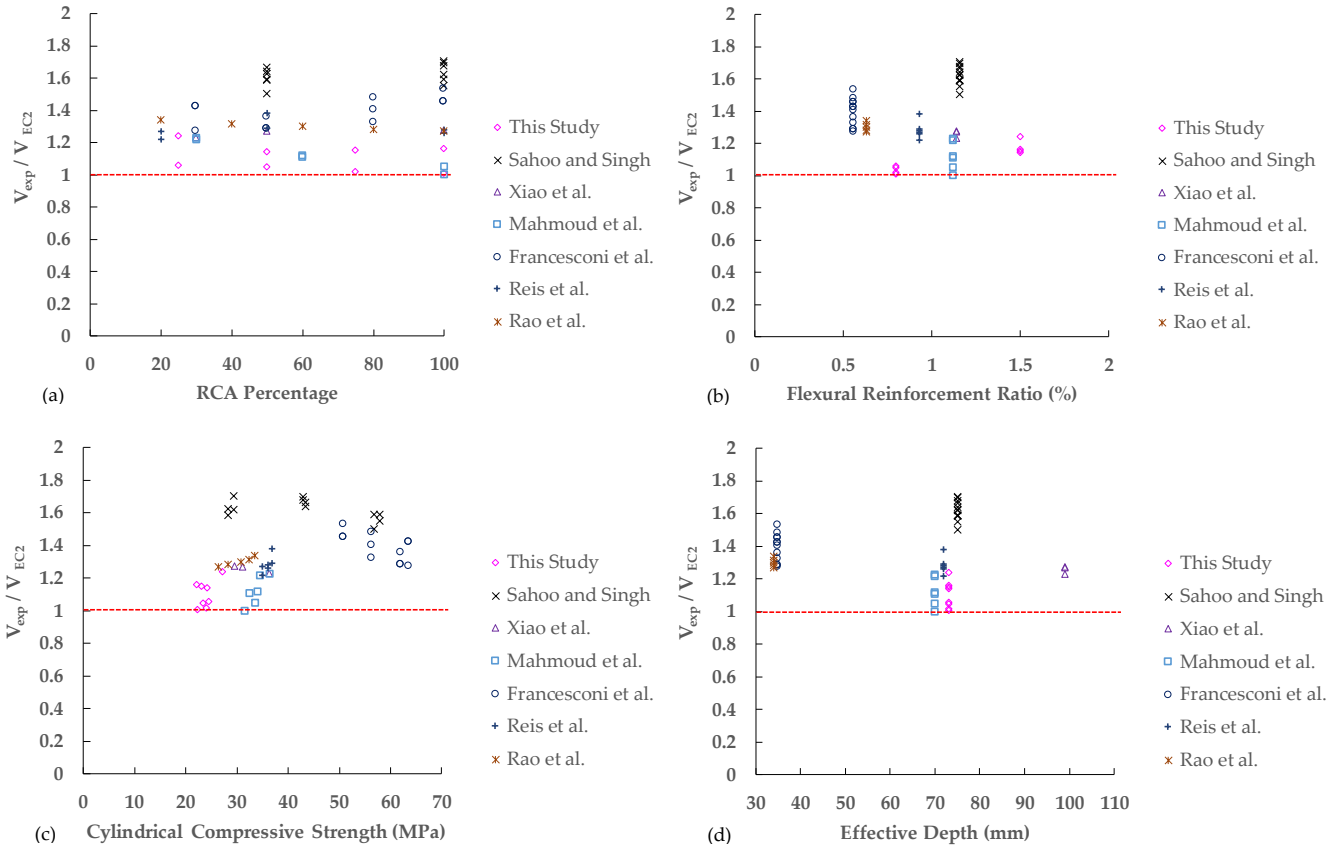

Figure 11. Eurocode 2 punching shear strength ratios versus (**a**) RCA percentage, (**b**) flexural reinforcement ratio, (**c**) cylindrical compressive strength, and (**d**) effective depth.

Most previous research studies were conducted using medium and high concrete compressive strength ranging from 30 to 69 MPa. This study investigated normal concrete compressive strength between 20 and 30 MPa, yielding conservative punching shear strength. However, ACI 318 can predict unconservative results for slabs with high strength concrete but low flexural reinforcement ratios, as shown in Figure 10c. Conversely, Eurocode 2 gives higher shear strength ratios, as shown in Figure 11c. For example, for slab RCA4-3 with 100% RCA, Eurocode 2 predicts 40% higher punching shear than ACI 318-19.

Effective depths (d) used in most tests are between 70 and 100 mm, except for 12 slabs with d less than 35 mm [40,42]. Again, Eurocode 2 generally provides more conservative results than ACI 318-19, as illustrated in Figures 10d and 11d.

3.5. Yield-Line Analysis

A yield-line analysis was carried out to estimate the flexural capacity of slabs. In this study, slabs were simply supported with all corners free to lift. The calculation was adapted from Elstner and Hognestad [51]. The shear force required to develop a flexural mechanism was calculated using the equation provided in Appendix A, as suggested in [52]. In this equation, the cylinder compressive strength and yield strength of flexural reinforcement were used, but the strain hardening of steel reinforcement was neglected. Table 6 and Figure 12 show the corresponding shear forces normalized by the yield-line loads.

Table 6. Comparison of punching shear capacity to yield-line load.

Specimen	V_{exp} (kN)	$V_{yield-line}$ (kN)	$V_{exp}/V_{yield-line}$
RCA-0-10	260.9	300.7	0.87
RCA-25-10	245.3	298.5	0.82
RCA-50-10	217.8	290.1	0.75
RCA-75-10	214.8	286.0	0.75
RCA-100-10	217.5	287.4	0.76
RCA-0-20	180	166.3	1.08
RCA-25-20	164	164.9	0.99
RCA-50-20	159.8	164.0	0.97
RCA-75-20	156.9	164.5	0.95
RCA-100-20	150.4	162.6	0.92

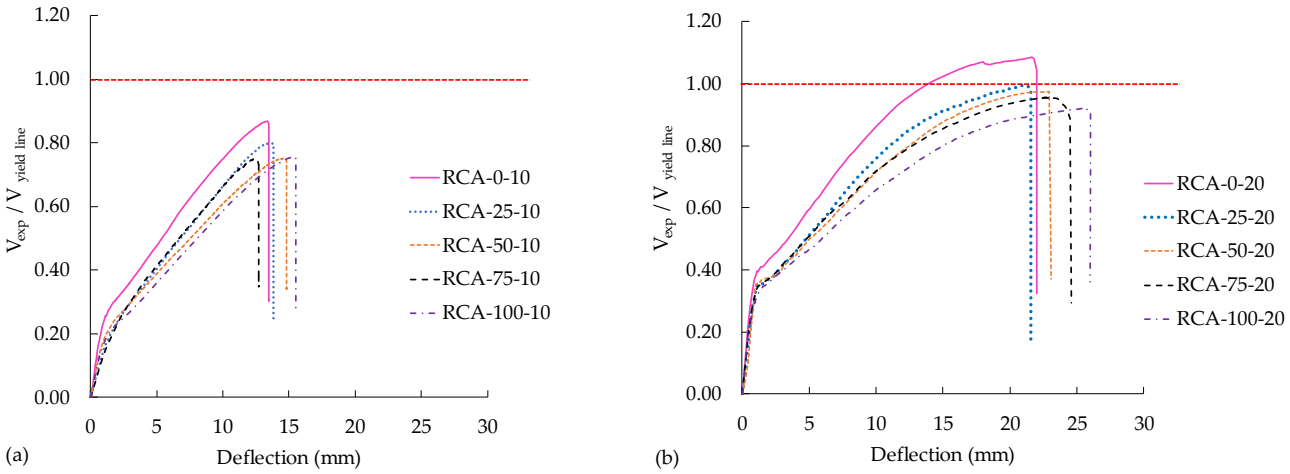

Figure 12. Shear normalized by yield-line load vs. deflection curves: (**a**) slabs with ρ = 1.5%; (**b**) slabs with ρ = 0.8%.

The ratios of experimental shear and yield-line load were used to confirm failure modes of the tested slabs. As the yield-line load is the predicted flexural capacity of the slab, the $V_{exp}/V_{yield-line}$ was less than 1, thus confirming punching shear failures of the slabs. In this study, the shear ratios were below 1 for slabs with ρ = 1.5%, thus indicating that slabs in this series failed in punching shear mode. For slabs with ρ = 0.8%, the controlled slab without RCA (RCA-0-20) had $V_{exp}/V_{yield-line}$ of 1.09, thus indicating flexural failure just before punching shear occurred. Other RAC slabs with ρ = 0.8% had $V_{exp}/V_{yield-line}$ ratios just below 1, thus suggesting a punching shear failure before a flexural failure.

4. Conclusions

This article experimentally investigated the performance of the punching shear of two-way slabs. Slabs were cast with recycled aggregate concrete (RAC) at replacement levels ranging from 25% to 100%. Two flexural reinforcement ratios of 0.8% and 1.5% were examined. From a database of 52 slabs tested in the literature, the experimental punching shear strength ratios were compared against ACI 318-19 and Eurocode 2 predictions. The following conclusions were drawn based on the results from this and previous studies:

- The normalized punching shear strength of 100% RAC slabs was lower than those of the NAC counterparts by 6.5% and 9% for flexural reinforcement ratios of ρ = 1.5% and 0.8%, respectively.
- Doubling the flexural reinforcement ratio increased the punching shear strength of RAC slabs by 45%.

- Based on the punching shear strength database, Eurocode 2 proved to give a more conservative prediction of punching shear strength with a mean shear strength ratio of 1.34, against a ratio of 1.39 given by ACI 318.
- Based on the database of punching shear strength, the ACI 318-19 can predict unconservative punching shear strengths for slabs with high concrete compressive strength but low flexural reinforcement ratios (ρ = 0.56%). The lowest shear strength ratio was 0.87, indicating a lower punching shear prediction (by 13%) compared to the test result.
- Except for slabs with a low reinforcement ratio below 0.6%, ACI 318-19 generally gives a conservative prediction for punching shear strength of RAC slabs at all levels of RCA contents.
- Based on the experimental evidence to date, both ACI 318-19 and Eurocode 2 can be used conservatively to predict the punching shear capacity of RAC slabs with reinforcement ratios greater than 0.6%.
- The yield-line analysis shows that RAC slabs failed by a punching shear mode, which is consistent with the test results.

5. Design Recommendation and Future Work

Based on the test results from this study and from other researchers, for slabs with a flexural reinforcement ratio not less than 0.6%, ACI 318-19 and Eurocode 2 can be used to predict the punching shear strength of RAC slabs at all levels of NCA substitution. However, for slabs with low flexural reinforcement ratios (less than 0.6%), Eurocode 2 is recommended to determine the punching shear capacity of RAC slabs. It should be noted that these calculations did not consider material partial factors, nor strength reduction factors. In the real design, these factors are included in the calculations, hence reducing the punching shear capacity and yielding much more conservative values.

As the present study is limited to RCA derived from old concrete with a compressive strength of around 30 MPa, and considering the complexity of shear behavior, further tests on slabs made from different qualities of RCA are necessary to fully validate the conclusions mentioned above. Furthermore, the effect of flexural reinforcement ratios below 0.6% on the punching shear capacity of RAC slabs should be reassessed considering tests on large-scale specimens, mainly because previous studies only focused on small-scale specimens.

Author Contributions: Conceptualization, M.S. and S.L.; methodology, M.S. and S.L.; validation, T.I., B.K. and R.G.; formal analysis, M.S. and S.L.; investigation, M.S., S.L., T.I., B.K. and R.G.; resources, S.L.; writing—original draft preparation, M.S. and S.L.; writing—review and editing, M.S., T.I., R.G. and B.K.; supervision, M.S.; funding acquisition, M.S. and S.L. All authors have read and agreed to the published version of the manuscript.

Funding: This research was funded by a Walailak University research grant (contract no. WU_IRG61_31).

Institutional Review Board Statement: Not applicable.

Informed Consent Statement: Not applicable.

Data Availability Statement: Not applicable.

Acknowledgments: The authors thankfully acknowledge Kiattisak Muangkaew, Tanawad Lengtoo, Surawit Channun, Phurichon Setchan, Atsawin Khonghom, and Wanlop Mankong who helped experimental works in the laboratory.

Conflicts of Interest: The authors declare no conflict of interest.

Appendix A

The punching shear strengths stipulated in ACI 319-19 and Eurocode (EC2) provisions are summarized as follows.

ACI 318-19

The ACI 318-19 [46] provision provides equations for the punching shear strength by the least of the following expressions:

$$V_{ACI} = \left\{ \begin{array}{c} 0.33\lambda_s \lambda \sqrt{f_c} b_o d \\ \left(0.17 + \frac{0.33}{\beta}\right) \lambda_s \lambda \sqrt{f_c} b_o d \\ \left(0.17 + \frac{0.083\alpha_s d}{b_o}\right) \lambda_s \lambda \sqrt{f_c} b_o d \end{array} \right\} \quad \text{(A1)}$$

where $\lambda_s = \sqrt{\frac{2}{1+0.004d}} \le 1$ is a size effect modification factor, which reduces the shear strength of two-way slabs when d > 250 mm; β is the ratio of long to short sides of the column; α_s = 40 for interior column; λ = 1 for normal weight concrete and 0.75 for light-weight concrete; f_c is the cylindrical compressive strength of concrete; d is the effective depth; and b_o is the perimeter of a critical section located at d/2 from the column faces. The perimeter b_o in ACI 318 is defined by assuming straight sides around the square or rectangular columns.

In this study, the column had a cross-section of 200 × 200 mm and d was 73 mm, resulting in b_o = 1092 mm. Taking λ = 1, α_s = 40, β = 1, and λ_s = 1 for this study, the smallest value of shear strength is $0.33\sqrt{f_c} b_o d$.

Eurocode 2

The punching shear capacity of slabs is estimated by the following equation.

$$V_{EC2} = C_{Rd,k} k \left(100 \cdot \rho \cdot f_c\right)^{1/3} b_o d \quad \ge \quad 0.035 k^{3/2} f_c^{1/2} b_o d \quad \text{(A2)}$$

where

$C_{Rd,k}$ = 0.18/γ_c;

γ_c = partial factor for concrete material;

d = effective depth of the slab, which is 73 mm in this study;

k = factor of the size effect = $1 + \sqrt{\frac{200}{d}} \le 2$;

f_c = cylindrical compressive strength of concrete;

ρ = flexural reinforcement ratio, which must be less than 0.002;

b_o = perimeter of a critical section located at the distance *2d* from the column face, which is $2(C_1 + C_2) + 4\pi d$, as shown in Figure A1.

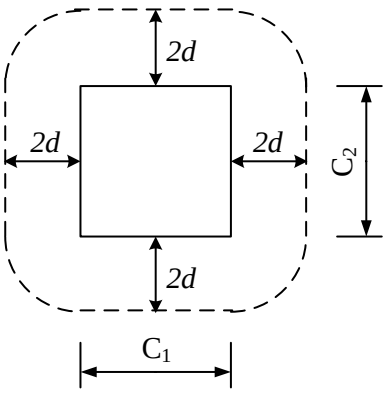

Figure A1. Perimeter of the critical section for punching shear based on Eurocode 2.

Yield-Line Analysis

Based on the virtual-work method, the yield-line load can be calculated from the following equation [52].

$$V = 8m\left(\frac{1}{1-\frac{r}{L}} - 3 + 2\sqrt{2}\right) \quad \text{(A3)}$$

$$m = \frac{A_s f_y\left(d - \frac{a}{2}\right)}{b}$$

$$a = \frac{A_s f_y}{0.85 b f_c^{'}}$$

where

r = side of the square column (mm);

L = width of the slab (mm);
b = spacing of flexural reinforcement;
d = effective depth of flexural reinforcement.

Example of the yield-line load for RAC-25-10:

r = 200 mm;
L = 1500 mm;
b = 100 mm;
d = 73 mm;
f_c' = 27.2 MPa;
f_y = 568.8 MPa;
A_s = 113 mm^2.

$$a = \frac{A_s f_y}{0.85 b f_c^{'}} = \frac{113 \times 568.8}{0.85 \times 100 \times 27.2} = 27.8\ mm$$

$$\beta = 0.85$$

$$c = a / \beta = 32.7\ \ mm$$

$$\varepsilon_s = \frac{d-c}{c} \times 0.003 = \frac{73 - 33.98}{33.98} \times 0.003 = 0.0037 \quad > \varepsilon_y$$

$$m = \frac{A_s f_y\left(d - \frac{a}{2}\right)}{b} = \frac{113 \times 568.8 \times \left(73 - \frac{27.8}{2}\right)}{100} = 37986\ N \cdot mm / mm$$

$$V = 8m\left(\frac{1}{1-\frac{r}{L}} - 3 + 2\sqrt{2}\right) = 8 \times 37986 \times \left(\frac{1}{1-\frac{200}{1500}} - 3 + 2\sqrt{2}\right) = 298501\ N = 298.5\ kN$$

References

1. Wang, B.; Yan, L.; Fu, Q.; Kasal, B. A comprehensive review on recycled aggregate and recycled aggregate concrete. *Resour. Conserv. Recycl.* **2021**, *171*, 105565.
2. Liew, K.M.; Sojobi, A.O.; Zhang, L.W. Green concrete: Prospects and challenges. *Constr. Build. Mater.* **2017**, *156*, 1063–1095. https://doi.org/10.1016/j.conbuildmat.2017.09.008.

3. Khatib, J.; Jahami, A.; Elkordi, A.; Baalbaki, O. Structural performance of reinforced concrete beams containing plastic waste caps. *Mag. Civ. Eng.* **2019**, *7*, 73–79.
4. Mohammed, A.A. Flexural behavior and analysis of reinforced concrete beams made of recycled PET waste concrete. *Constr. Build. Mater.* **2017**, *155*, 593–604.
5. Tam, V.W.Y.; Soomro, M.; Evangelista, A.C.J. A review of recycled aggregate in concrete applications (2000–2017). *Constr. Build. Mater.* **2018**, *172*, 272–292. https://doi.org/10.1016/j.conbuildmat.2018.03.240.
6. Makul, N.; Fediuk, R.; Mugahed Amran, H.; Zeyad, A.M.; de Azevedo, A.R.G.; Klyuev, S.; Vatin, N.; Karelina, M. Capacity to Develop Recycled Aggregate Concrete in South East Asia. *Buildings* **2021**, *11*, 234.
7. Kisku, N.; Joshi, H.; Ansari, M.; Panda, S.; Nayak, S.; Dutta, S.C. A critical review and assessment for usage of recycled aggregate as sustainable construction material. *Constr. Build. Mater.* **2017**, *131*, 721–740.
8. Sunayana, S.; Barai, S.V. Flexural performance and tension-stiffening evaluation of reinforced concrete beam incorporating recycled aggregate and fly ash. *Constr. Build. Mater.* **2018**, *174*, 210–223. https://doi.org/10.1016/j.conbuildmat.2018.04.072.
9. Seara-Paz, S.; González-Fonteboa, B.; Martínez-Abella, F.; Eiras-López, J. Flexural performance of reinforced concrete beams made with recycled concrete coarse aggregate. *Eng. Struct.* **2018**, *156*, 32–45. https://doi.org/10.1016/j.engstruct.2017.11.015.
10. Arezoumandi, M.; Smith, A.; Volz, J.S.; Khayat, K.H. An experimental study on flexural strength of reinforced concrete beams with 100% recycled concrete aggregate. *Eng. Struct.* **2015**, *88*, 154–162. https://doi.org/10.1016/j.engstruct.2015.01.043.
11. Ignjatović, I.S.; Marinković, S.B.; Mišković, Z.M.; Savić, A.R. Flexural behavior of reinforced recycled aggregate concrete beams under short-term loading. *Mater. Struct.* **2013**, *46*, 1045–1059.
12. Choi, W.-C.; Yun, H.-D. Long-term deflection and flexural behavior of reinforced concrete beams with recycled aggregate. *Mater. Des.* **2013**, *51*, 742–750. https://doi.org/10.1016/j.matdes.2013.04.044.
13. Song, S.-H.; Choi, K.-S.; You, Y.-C.; Kim, K.-H.; Yun, H.-D. Flexural behavior of reinforced recycled aggregate concrete beams. *J. Korea Concr. Inst.* **2009**, *21*, 431–439.
14. Ajdukiewicz, A.B.; Kliszczewicz, A.T. Comparative tests of beams and columns made of recycled aggregate concrete and natural aggregate concrete. *J. Adv. Concr. Technol.* **2007**, *5*, 259–273.
15. Yu, F.; Wang, M.; Yao, D.; Yang, W. Study on Flexural Behavior of Self-Compacting Concrete Beams with Recycled Aggregates. *Buildings* **2022**, *12*, 881.
16. Setkit, M.; Leelatanon, S.; Imjai, T.; Garcia, R.; Limkatanyu, S. Prediction of Shear Strength of Reinforced Recycled Aggregate Concrete Beams without Stirrups. *Buildings* **2021**, *11*, 402.
17. Wardeh, G.; Ghorbel, E. Shear strength of reinforced concrete beams with recycled aggregates. *Adv. Struct. Eng.* **2019**, *21*, 1369433219829815.
18. Rahal, K.N.; Alrefaei, Y.T. Shear strength of recycled aggregate concrete beams containing stirrups. *Constr. Build. Mater.* **2018**, *191*, 866–876. https://doi.org/10.1016/j.conbuildmat.2018.10.023.
19. Pradhan, S.; Kumar, S.; Barai, S.V. Shear performance of recycled aggregate concrete beams: An insight for design aspects. *Constr. Build. Mater.* **2018**, *178*, 593–611.
20. Etman, E.E.; Afefy, H.M.; Baraghith, A.T.; Khedr, S.A. Improving the shear performance of reinforced concrete beams made of recycled coarse aggregate. *Constr. Build. Mater.* **2018**, *185*, 310–324. https://doi.org/10.1016/j.conbuildmat.2018.07.065.
21. Rahal, K.; Alrefaei, Y. Shear strength of longitudinally reinforced recycled aggregate concrete beams. *Eng. Struct.* **2017**, *145*, 273–282.
22. Ignjatović, I.S.; Marinković, S.B.; Tošić, N. Shear behaviour of recycled aggregate concrete beams with and without shear reinforcement. *Eng. Struct.* **2017**, *141*, 386–401.
23. Choi, W.-C.; Yun, H.-D. Shear strength of reinforced recycled aggregate concrete beams without shear reinforcements. *J. Civ. Eng. Manag.* **2017**, *23*, 76–84.
24. Tošić, N.; Marinković, S.; Ignjatović, I. A database on flexural and shear strength of reinforced recycled aggregate concrete beams and comparison to Eurocode 2 predictions. *Constr. Build. Mater.* **2016**, *127*, 932–944.
25. Sadati, S.; Arezoumandi, M.; Khayat, K.H.; Volz, J.S. Shear performance of reinforced concrete beams incorporating recycled concrete aggregate and high-volume fly ash. *J. Clean. Prod.* **2016**, *115*, 284–293.
26. Katkhuda, H.; Shatarat, N. Shear behavior of reinforced concrete beams using treated recycled concrete aggregate. *Constr. Build. Mater.* **2016**, *125*, 63–71.
27. Arezoumandi, M.; Drury, J.; Volz, J.S.; Khayat, K.H. Effect of recycled concrete aggregate replacement level on shear strength of reinforced concrete beams. *ACI Mater. J.* **2015**, *112*, 559.
28. Knaack, A.M.; Kurama, Y.C. Behavior of reinforced concrete beams with recycled concrete coarse aggregates. *J. Struct. Eng.* **2014**, *141*, B4014009.
29. Arezoumandi, M.; Smith, A.; Volz, J.S.; Khayat, K.H. An experimental study on shear strength of reinforced concrete beams with 100% recycled concrete aggregate. *Constr. Build. Mater.* **2014**, *53*, 612–620. https://doi.org/10.1016/j.conbuildmat.2013.12.019.
30. Kim, S.-W.; Jeong, C.-Y.; Lee, J.-S.; Kim, K.-H. Size effect in shear failure of reinforced concrete beams with recycled aggregate. *J. Asian Archit. Build. Eng.* **2013**, *12*, 323–330.
31. Fathifazl, G.; Razaqpur, A.G.; Burkan Isgor, O.; Abbas, A.; Fournier, B.; Foo, S. Shear capacity evaluation of steel reinforced recycled concrete (RRC) beams. *Eng. Struct.* **2011**, *33*, 1025–1033. https://doi.org/10.1016/j.engstruct.2010.12.025.
32. Choi, H.; Yi, C.; Cho, H.; Kang, K. Experimental study on the shear strength of recycled aggregate concrete beams. *Mag. Concr. Res.* **2010**, *62*, 103–114.

33. González-Fonteboa, B.; Martínez-Abella, F.; Martínez-Lage, I.; Eiras-López, J. Structural shear behaviour of recycled concrete with silica fume. *Constr. Build. Mater.* **2009**, *23*, 3406–3410. https://doi.org/10.1016/j.conbuildmat.2009.06.035.
34. Sato, R.; Maruyama, I.; Sogabe, T.; Sogo, M. Flexural behavior of reinforced recycled concrete beams. *J. Adv. Concr. Technol.* **2007**, *5*, 43–61.
35. González-Fonteboa, B.; Martínez-Abella, F. Shear strength of recycled concrete beams. *Constr. Build. Mater.* **2007**, *21*, 887–893. https://doi.org/10.1016/j.conbuildmat.2005.12.018.
36. Etxeberria, M.; Mari, A.; Vazquez, E. Recycled aggregate concrete as structural material. *Mater. Struct.* **2007**, *40*, 529–541.
37. Sogo, M.; Sogabe, T.; Maruyama, I.; Sato, R.; Kawai, K. Shear behavior of reinforced recycled concrete beams. In Proceedings of the International RILEM Conference on the Use of Recycled Materials in Buildings and Structures, Barcelona, Spain, 8–11 November 2004; pp. 8–11.
38. Han, B.; Yun, H.; Chung, S. Shear capacity of reinforced concrete beams made with recycled-aggregate. *Spec. Publ.* **2001**, *200*, 503–516.
39. Rahal, K.N.; Elsayed, K. Shear strength of 50 MPa longitudinally reinforced concrete beams made with coarse aggregates from low strength recycled waste concrete. *Constr. Build. Mater.* **2021**, *286*, 122835.
40. Rao, H.S.; Reddy, V.S.K.; Ghorpade, V.G. Influence of recycled coarse aggregate on punching behaviour of recycled coarse aggregate concrete slabs. *Environment* **2012**, *6*, 7.
41. Reis, N.; de Brito, J.; Correia, J.R.; Arruda, M.R.T. Punching behaviour of concrete slabs incorporating coarse recycled concrete aggregates. *Eng. Struct.* **2015**, *100*, 238–248. https://doi.org/10.1016/j.engstruct.2015.06.011.
42. Francesconi, L.; Pani, L.; Stochino, F. Punching shear strength of reinforced recycled concrete slabs. *Constr. Build. Mater.* **2016**, *127*, 248–263. https://doi.org/10.1016/j.conbuildmat.2016.09.094.
43. Mahmoud, Z.I.; El tony, E.t.M.; Saeed, K.S. Punching shear behavior of recycled aggregate reinforced concrete slabs. *Alex. Eng. J.* **2018**, *57*, 841–849. https://doi.org/10.1016/j.aej.2015.12.004.
44. Xiao, J.; Wang, W.; Zhou, Z.; Tawana, M.M. Punching shear behavior of recycled aggregate concrete slabs with and without steel fibres. *Front. Struct. Civ. Eng.* **2019**, *13*, 725–740.
45. Sahoo, S.; Singh, B. Punching shear capacity of recycled-aggregate concrete slab-column connections. *J. Build. Eng.* **2021**, *41*, 102430.
46. *ACI 318-19*; Building Code Requirements for Structural Concrete and Commentary. American Concrete Institute: Farmington Hills, MI, USA, 2019.
47. *EN-1992-1-1*; Eurocode 2: Design of Concrete Structures—Part 1-1: General Rules and Rules for Buildings. British Standard Institution: London, UK, 2004; pp. 97–105.
48. ASTM International. Standard Test Method for Sieve Analysis of Fine and Coarse Aggregates, (ASTM C136/C136M-19). 2019. West Conshohocken, PA.
49. ACI 211.1-91; Standard Practice for Selecting Proportions for Normal, Heavy Weight and Mass Concrete. American Concrete Institute. Famington Hills, MI, USA, 2002.
50. Teng, S.; Chanthabouala, K.; Lim, D.T.; Hidayat, R. Punching Shear Strength of Slabs and Influence of Low Reinforcement Ratio. *ACI Struct. J.* **2018**, *115*, 139-A128.
51. Elstner, R.C.; Hognestad, E. Shearing strength of reinforced concrete slabs. In Journal Proceedings, 1956, 53, 29-58.
52. Cheng, M.-Y. Punching Shear Strength and Deformation Capacity of Fiber Reinforced Concrete Slab-Column Connections under Earthquake-Type Loading. Ph.D. Dissertation, University of Michiagan, Ann Arbor, MI, USA, 2008.